The Role of Cerium Sites in the Scintillation Mechanism of LSO

J. D. Naud and T. A. Tombrello
Division of Physics, Mathematics, and Astronomy,
California Institute of Technology, Pasadena, CA 91125

C. L. Melcher and J. S. Schweitzer
Schlumberger-Doll Research, Old Quarry Road, Ridgefield, CT 06877-4108

Abstract

The crystal structure of $Lu_2(SiO_4)O$:Ce ("LSO") has two trivalent cation sites which may be occupied by Ce^{3+} to form luminescence centers. Previous investigations revealed the existence of two distinct sets of Ce^{3+} excitation and emission spectra and suggested that the differences in the spectra are due to differences in the crystal fields at the two lattice sites that shift the 5d levels of Ce^{3+}. In the present report, we re-examine this issue and present new evidence which suggests a different interpretation. In particular, spectra measured at 13 K suggest that both lattice sites give rise to indistinguishable excitation and emission spectra while the second set of observed spectra arises from Ce^{3+} located in interstitial sites. The evidence for the interstitial sites is a disappearance of the doublet structure in the emission spectra and a large variation in the population of the sites as a function of total cerium concentration. In addition, the results indicate that the scintillation properties of LSO are influenced by the relative population of Ce in interstitial sites compared to lattice sites as well as by differences in the transfer efficiencies to different sites.

I. Introduction

The host material of LSO is $Lu_2(SiO_4)O$, which has a monoclinic structure of space group C2/c, and is a good insulator, with a band gap energy of approximately 6 eV. In this lattice, the Lu atoms occupy two equally-populated, crystallographically independent sites, which have oxygen coordination numbers of 6 and 7, and average nearest-neighbor distances of 2.22 Å and 2.32 Å, respectively [1]. When doped with cerium, the Ce substitutes for the Lu. Ce^{3+} possesses a single valence electron in the 4f level, which can be excited into the 5d level. The 5d level is split by the crystal field of the host lattice into 3 sublevels, and the 4f ground state is split by the spin-orbit interaction into two levels, with an energy separation of 2253 cm^{-1}[2]. The luminescence of LSO is due to parity-allowed electric dipole transitions from the lowest 5d sublevel to the split 4f ground state.

Under UV-excitation LSO exhibits two distinct types of excitation and emission spectra. Since there are two crystallographically independent lutetium sites in the host lattice into which the Ce can substitute, a two-activation-center model has been proposed in which the two sets of excitation and emission spectra are identified with Ce^{3+} substituted at the two different Lu sites, designated Ce1 and Ce2 [3].

The motivation for the present investigation is the variation observed in the scintillation and luminescent properties of LSO crystals produced under a variety of growth conditions and with different cerium concentrations. Although LSO crystals grown under optimal conditions and with optimal cerium concentrations have high light output (>20,000 ph/MeV), the light output of other LSO crystals may be as much as an order of magnitude less. In addition to the total room temperature light output, the temperature dependence of the gamma-ray-excited light output is observed to vary from crystal to crystal.

II. Experiment

All the samples used in this study were grown by the Czochralski technique which is described elsewhere [4]. The concentration of Ce in the melts from which the crystals were grown varied from boule to boule. The distribution coefficient of Ce in LSO is relatively low, approximately 0.22, due to the large difference in ionic radii between the host Lu^{3+} (0.848 Å) and the dopant Ce^{3+} (1.034 Å) [4]. Since the experimentally determined distribution coefficient is relatively uniform over a wide range of Ce melt concentrations, we assume that for all LSO samples the concentration of Ce in a given crystal is proportional to the concentration of Ce in the corresponding melt.

The set of samples chosen for this study is given in Table 1. The light output is from gamma-ray-excitation at room temperature. The seven LSO samples were chosen to represent the extremes in Ce concentrations and room temperature light outputs observed among all the crystals grown to date.

As noted above, LSO exhibits two distinct types of luminescent spectra, Ce1 and Ce2. At temperatures above ~80 K, thermal broadening causes a significant overlap of the Ce1 and Ce2 excitation bands; it becomes difficult to selectively

Table 1. Results for the set of LSO crystals studied.

Sample	Ce conc.	Light Output	R_{UV}	R_{GR}	T_Q (K)	E_A (eV)
LSO 73	0.10	2.19	5.67	0.487	361	0.406
LSO 57	0.54	1.80	4.48	0.158	329	0.370
LSO 84	0.05	1.60	24.9	0.0975	339	0.411
LSO 44	0.55	1.09	4.08	0.163	322	0.368
LSO 27	0.25	0.85	4.11	0.610	318	0.365
LSO 34	2.12	0.58	3.18	0.147	309	0.328
LSO 25	0.50	0.28	5.09	0.551	316	0.333

0-7803-3180-X/96$5.00©1996

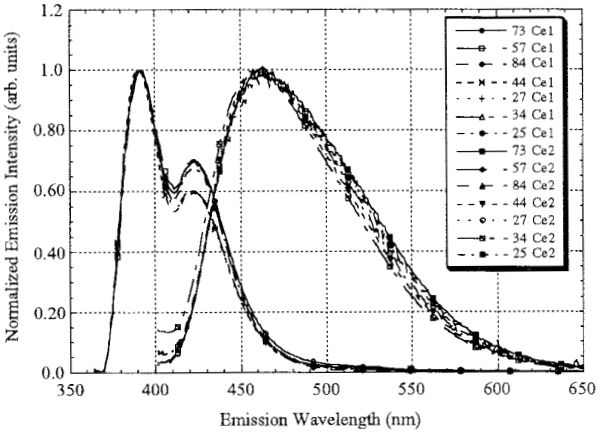

Figure 1. Normalized Ce1 emission spectra (excited at 356 nm) and Ce2 emission spectra (excited at 376 nm) at 13 K. Each spectrum is normalized to its peak intensity.

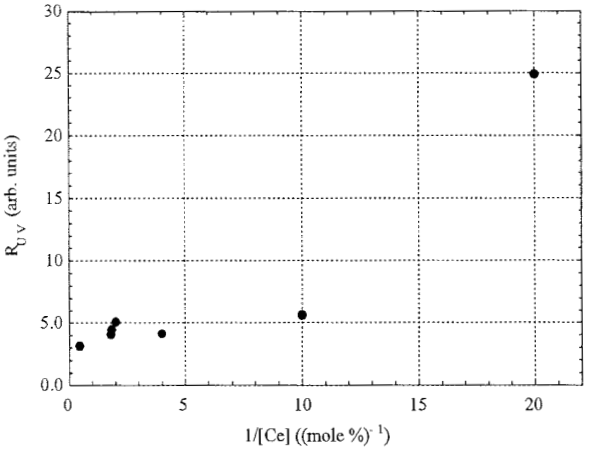

Figure 2. Measure of the ratio of concentrations of Ce1 and Ce2 as a function of the reciprocal of the total Ce concentration.

excite either center independently [3]. Hence, to resolve the two types of luminescence, we performed measurements at low temperature. The crystals (1x1x1 cm^3) were mounted on the cold station of a CTI-Cryogenics refrigeration system (Model 21). The temperature was controlled by a nichrome heater wire (NC-32, Lakeshore Electronics) and monitored by a silicon diode sensor (CY7-CU4, OMEGA Electronics) mounted on the copper sample holder. The samples were maintained at a temperature of 13 ± 1 K during the measurements. The refrigeration system was incorporated in a SPEX Fluorolog-2 spectrofluorometer. For the UV-excited measurements, the light source was an ozone-free 450 W high pressure xenon lamp. Double monochrometers were used in both the excitation and emission paths. For the UV-excited measurements, the excitation beam was normally incident on one face of the crystal, and the luminescent emission was measured at an angle of 22.5 ° from the normal. For the gamma-ray-excited measurements, the configuration was the same except that an uncollimated ^{241}Am source was placed ~2 cm from the sample. The band pass was 0.9 nm for the UV-excited measurements and 2.7 nm for the gamma-ray-excited measurements.

In addition to these low temperature photoluminescence measurements, we investigated the temperature dependence of the gamma-ray-excited light output of the crystals. Each sample was coupled to a photomultiplier tube (PMT), and the assembly was placed inside a temperature controlled chamber along with a ^{137}Cs source. Before any data were taken, each crystal was heated to 150 °C inside the chamber to empty any thermoluminescent traps, so that any thermoluminescent emission intensity would be small compared with the gamma-ray-excited emission intensity. Measurements were taken at ~25 °C intervals between -38 °C and 150 °C. The experimental data were then corrected for the temperature response of the PMT in order to provide the temperature variation of the scintillation efficiency of the crystal.

III. Results

The Ce1 emission spectrum of each sample was measured at 13 K using an excitation wavelength of 356 nm, corresponding to the strongest Ce1 excitation band [3]. The Ce1 emission spectra at 13 K, normalized to their peak intensities are given in Figure 1. Emission peaks appear at 393 and 427 nm. The doublet structure of the spectra is due to transitions of the Ce^{3+} ion from the lowest 5d level to the 4f ground and first excited states [3]. The emission spectra all possess very similar shapes; the only difference between them is the relative height of the lower energy peak.

The Ce2 emission spectra were measured at 13 K by exciting the samples at 376 nm, the location of the strongest Ce2 excitation band; they are shown in Figure 1 normalized to their peak intensities. The Ce2 spectra are considerably wider than the Ce1 spectra, having a FWHM of approximately 100 nm compared to a FWHM of about 60 nm for Ce1. The doublet structure due to the presence of the two Ce^{3+} 4f states is not observed in these spectra. In addition, there is more variation in the shapes of the normalized Ce2 spectra than in the shapes of the normalized Ce1 spectra.

We assume that the integral of the emission intensity from a given type of Ce center is directly proportional to the concentration of that type of Ce center, at least over the range of total cerium concentrations investigated in this study. Therefore, the ratio of the concentrations of the two classes of Ce centers in a sample is proportional to the ratio of the sample's integrated emission intensities from the two types of Ce centers. For each crystal, we integrated the low temperature, unnormalized Ce1 and Ce2 emission spectra and took the ratio of the integrals, R_{UV}, as a measure of [Ce1]/[Ce2]. The results are given in Table 1. Note that R_{UV} varies over a range of almost a factor of eight. In Figure 2 we observe that the ratio of concentrations is correlated with the reciprocal of the total Ce concentration in the crystal.

The gamma-ray-excited emission spectra at 13 K, normalized to their peak intensities, are given in Figure 3; two different types of spectral shapes are observed. LSO 34, 44, and 57 exhibit considerably more emission above 425 nm than the other samples in the study. To investigate the cause of this difference, we define $f_1(\lambda)$ and $f_2(\lambda)$ as the low temperature spectral shape functions for UV-excited Ce1 and Ce2 emission, respectively. Based on Figure 1 we make the approximation that $f_1(\lambda)$ and $f_2(\lambda)$ are independent of the

sample. Given our assumption in the preceding paragraph, the 13 K UV-excited emission spectrum of Ce(i) is given by:

$$UV_i(\lambda) = k_i[Ce(i)]f_i(\lambda) \qquad i = 1, 2\,, \tag{1}$$

where k_1 and k_2 are constants, independent of the sample. Similarly, the gamma-ray-excited low temperature spectrum is:

$$GR(\lambda) = k_3\eta(\lambda)\,, \tag{2}$$

where k_3 is a constant, and $\eta(\lambda)$ is the scintillation efficiency at 13 K. The scintillation efficiency can be written as [5]:

$$\eta(\lambda) = \beta(S_1Q_1[Ce1]f_1(\lambda) + S_2Q_2[Ce2]f_2(\lambda))\,, \tag{3}$$

where β is the low temperature conversion efficiency, and $S_{1(2)}$ and $Q_{1(2)}$ are the low temperature transfer and luminescent efficiencies for Ce1(2), respectively. At 13 K we assume the quantum efficiency of the luminescent centers to be unity: $Q_1 = Q_2 = 1$. Hence, (1), (2) and (3) give:

$$GR(\lambda) = C_1(R_{GR}UV_1(\lambda) + UV_2(\lambda))\,, \tag{4}$$

where $C_1 = (\beta S_2 k_3)/k_2$ and

$$R_{GR} = (k_2/k_1)(S_1/S_2) \tag{5}$$

Hence, the quantity R_{GR} is proportional to the ratio of the low temperature transfer efficiencies of the two Ce centers. From (4) it is clear that if we fit the gamma-ray-excited emission spectrum of each sample as a weighted sum of the UV-excited Ce1 and Ce2 spectra of the sample, the ratio of the best-fit weights will yield R_{GR}. An example of the resulting fit, for LSO 44, is given in Figure 4. Note the close agreement between the gamma-ray-excited spectrum and the weighted combination of the UV-excited Ce1 and Ce2 spectra. The agreement for the other samples was at least as good as that demonstrated in Figure 4. The calculated values of R_{GR} for each sample are given in Table 1. The results clearly indicate that the low temperature relative transfer efficiency, S_1/S_2, is not uniform among the samples. Based on the values of R_{GR} we can divide the LSO samples into three general groups: LSO 84 with $R_{GR} \sim 0.1$, LSO 57, 44, and 34 with $R_{GR} \sim 0.15$ and LSO 73, 27, and 25 with $R_{GR} \sim 0.55$.

We now turn our attention to the temperature dependence of the gamma-ray-excited light output of the samples. The experimental data were fit to a Mott-Gurney equation, which is based on a simple three-level model (ground, excited, and quenching) of the luminescent center [6]:

$$L(T) = A_3/(1 + A_1\exp(-A_2/T))\,, \tag{6}$$

where L is the light output, T is the temperature, and A_1, A_2, and A_3 are parameters of the fit. In this model, A_1 is a measure of the relative probabilities of nonradiative and radiative transitions from the excited state of the center to the ground state, A_2 is equal to the energy difference between the excited state and a quenching state (divided by Boltzmann's constant, k_b), and A_3 is an overall normalization.

The best-fit curves suggest that, below approximately 250 K, the light output becomes essentially independent of temperature. Hence we can use the fit parameters to extrapolate the light output of each crystal to 0 K. From equation (6), the 0 K light output is A_3. The extrapolated 0 K light outputs of the samples obtained in this way are in good agreement with the light outputs at 13 K obtained by integrating the low temperature gamma-ray-excited emission spectra (shown normalized in Figure 3). This agreement suggests that the fits are reliable, and that the gamma-ray-excited light output is indeed essentially constant below 250 K.

Using the extrapolated 0 K light outputs, we can normalize the temperature response data for each sample to the 0 K value and then refit the data with equation (6), this time constraining A_3 to be 1. The results are given in Figure 5. The normalized curves for the LSO samples all possess the same shape; they appear to be just translations of one another. This suggests that the temperature response of each crystal can be approximated by a single parameter. We define this parameter, the quenching temperature, as the temperature at which the crystal's light output is equal to one half its 0 K

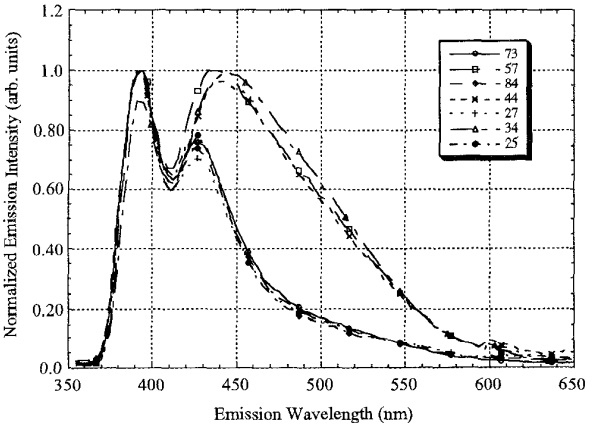

Figure 3. Normalized gamma-ray-excited emission spectra at 13 K. Each spectrum is normalized to its peak intensity.

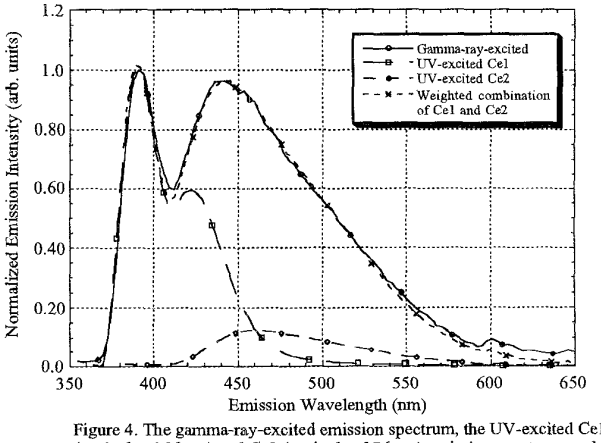

Figure 4. The gamma-ray-excited emission spectrum, the UV-excited Ce1 (excited at 356 nm) and Ce2 (excited at 376 nm) emission spectrum, and a weighted combination of the Ce1 and Ce2 emission spectra for LSO 44 at 13 K.

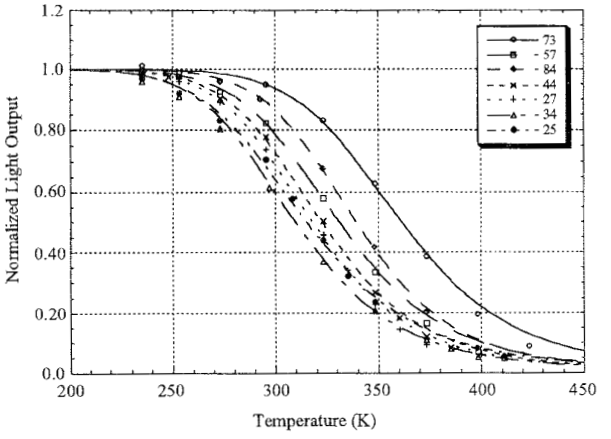

Figure 5. Normalized gamma-ray-excited light output as a function of temperature. The light output for each sample is normalized to 1 at 0 K.

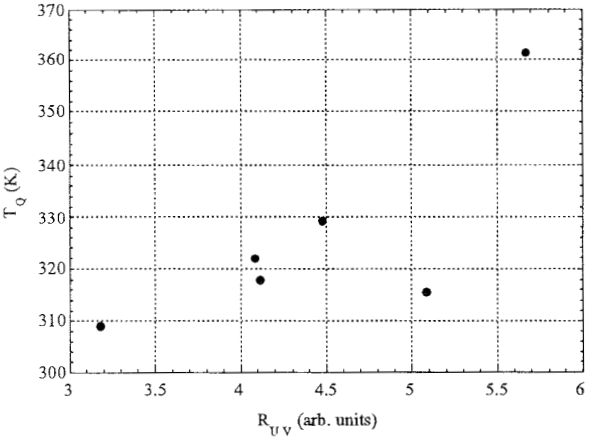

Figure 6. Quenching temperature as a function of the measure of the ratio of concentrations of Ce1 and Ce2 (LSO 84 not shown).

value. From equation (6), the quenching temperature, T_Q, is related to the fit parameters by:

$$T_Q = A_2/\log(A_1) \quad (7)$$

The calculated quenching temperatures are given in Table 1, along with the activation energies $E_A = k_b A_2$. In Figure 6 we plot the quenching temperature versus R_{UV}, the measure of [Ce1]/[Ce2], for the LSO samples. We observe that, with the exception of LSO 84, T_Q appears to be correlated with R_{UV}.

IV. Discussion

The current two-activation-center model of Suzuki et al. of the scintillation mechanism in LSO attributes the two distinct types of UV-excited excitation and emission spectra to Ce substituted at the two crystallographically independent Lu sites. We propose an alternate model in which the Ce1 luminescence is due to Ce substituted at either Lu lattice site, and the Ce2 luminescence is due to interstitial Ce centers. There are several observations in support of this alternate model. First, we clearly observe the spin-orbit splitting of the Ce^{3+} 4f ground state in the Ce1 emission spectra, while we see no such splitting in the Ce2 emission spectra (Figure 1). If the Ce2 emission corresponded to Ce substituted at a definite lattice site, like Ce1, there is no obvious explanation for the absence of the doublet structure in the low temperature emission spectra. However, if the Ce2 emission is due to Ce centers occupying a variety of slightly different interstitial sites, then the variation in the crystal field among these different sites may cause a spread in the energies of the Ce^{3+} 5d levels. Therefore, the spin-orbit splitting of the ground state in the Ce2 emission would be "washed-out" because of the range in energy of the lowest 5d level. This interpretation is also consistent with the greater width and sample to sample variation seen in the Ce2 emission spectra as compared with the Ce1 emission spectra.

A second observation in support of the existence of interstitial Ce centers is the variation seen in R_{UV}, which is a measure of [Ce1]/[Ce2], and its dependence on the total Ce concentration. Figure 2 indicates that the Ce^{3+} ions in the melt have a significantly easier time becoming Ce1 centers than Ce2 centers, to such a degree that the Ce2 emission can be essentially eliminated by going to low enough Ce concentrations, e.g. LSO 84. This suggests that the difference between the Ce1 and Ce2 sites is greater than the difference between the two Lu lattice sites, which differ only slightly in oxygen coordination number (6 and 7) and by only ~4% in average nearest-neighbor distance.

Third, recent work-in-progress on the numerical calculation of the energy levels of Ce^{3+} centers in LSO has found little difference in the 4f and 5d energy levels between the two Lu lattice sites [1],[7]. This suggests that the luminescent spectra from Ce at these two types of lattice sites would be very similar, and therefore supports our identification of the Ce1 spectra as arising from Ce substituted at either Lu lattice site.

Independent of whether the Ce2 emission is attributed to Ce at a Lu lattice site or interstitial Ce, the results of this investigation clearly indicate that both the low temperature ratio of UV-excited integrated emission intensities, R_{UV}, and the low temperature ratio of transfer efficiencies, R_{GR}, vary from sample to sample. These variations can be used, to some extent, to explain some of the observed differences in the scintillation properties among the samples. For example, the product $R_{UV}R_{GR}$, which is proportional to $([Ce1]S_1)/([Ce2]S_2)$ is equal to ~2.4-2.8 for all the LSO samples except LSO 34, 44, and 57, for which it is ~0.5-0.7. This result suggests that the difference in shape between the low temperature gamma-ray-excited spectra of LSO 34, 44, and 57, and the remaining LSO samples (Figure 3) is due to a combination of the effects of having more Ce2 relative to Ce1, and a larger value of S_2 relative to S_1 in these samples, as compared to the other LSO crystals.

The correlation between the quenching temperature of the gamma-ray-excited emission intensity and R_{UV} (Figure 6) suggests that Ce1 and Ce2 centers have different temperature responses, and hence the ratio [Ce1]/[Ce2] influences the temperature dependence of the overall light output. We note that while LSO 84 is not consistent with the trend visible in Figure 6, it does possess the highest activation energy of any sample investigated. The reason it does not possess a correspondingly high quenching temperature is that the fit

parameter A_1 is a factor of ~5 larger for LSO 84 than for any other LSO sample, suggesting that nonradiative processes are more prevalent in LSO 84 than in the other crystals.

V. Acknowledgments

We are grateful to R.A. Manente for growing the crystals used in this study.

VI. References

[1] J. Andriessen, A. Sobolev, A. Kuznetsov, H. Merenga, P. Dorenbos, and C. W. E. van Eijk, "Theoretical investigation of the 4f and 5d levels of cerium in LSO, studied with HF-LCAO and the embedded cluster scattered wave method," to be published.

[2] H. Suzuki, "Scintillation mechanisms of cerium-doped rare earth oxyorthosilicates," California Institute of Technology, Pasadena, CA, Ph.D. dissertation (1994).

[3] H. Suzuki, T. A. Tombrello, C. L. Melcher, and J. S. Schweitzer, "Light emission mechanism of $Lu_2(SiO_4)O$:Ce," *IEEE Trans. on Nucl. Science*, **40**, 380-383 (1993).

[4] C. L. Melcher, R. A. Manente, C. A. Peterson, and J. S. Schweitzer, "Czochralski growth of rare earth oxyorthosilicate single crystals," *J. of Crystal Growth*, **128**, 1001-1005 (1993).

[5] A. Lempicki, A. J. Wojtowicz and E. Berman, "Fundamental limits of scintillator performance," *Nucl. Inst. and Meth.*, **A333**, 304-311 (1993).

[6] J. B. Birks, *The theory and practice of scintillation counting*, New York: Macmillan, 459-460 (1964).

[7] J. Andriessen, P. Dorenbos, C. W. E. van Eijk, "Calculation of energy levels of cerium in inorganic scintillator crystals," *Mat. Res. Soc. Symp. Proc.*, **348**, 355 (1994).